A high-order model for in-plane vibrations of rotating rings on elastic foundation

Lu, Tao; Tsouvalas, Apostolos; Metrikine, Andrei

Important note
To cite this publication, please use the final published version (if applicable).
Please check the document version above.

A high-order model for in-plane vibrations of rotating rings on elastic foundation

T. Lu[*], A. Tsouvalas, A.V. Metrikine

Faculty of Civil Engineering and Geosciences, Delft University of Technology, Stevinweg 1, 2628 CN Delft, The Netherlands

Abstract

A new high-order model for in-plane vibrations of rotating rings is developed in this paper. The inner surface of the ring is connected to an immovable axis through an elastic foundation (distributed springs), whereas the outer surface is traction free. The developed model enables the dynamic analysis of the rings on stiff elastic foundation that rotate with a high speed. The traction force at the inner surface of such rings is so high that it influences significantly the through-thickness stress distribution. This boundary effect cannot be captured by the classical low order theories while the model proposed in this paper can account for this effect. Nonlinear equations of motion are first derived, considering the geometrical nonlinearity of the system while assuming the linear elastic behaviour of the ring material. The formulation accounts for the stress caused by rotation and the significant normal and tangential traction forces at the inner surface of the ring. The displacement fields are assumed to be polynomials of the through-thickness coordinate in both the radial and circumferential directions. The derivation is generic and can yield ring theories of different order, i.e. of the Timoshenko-type and beyond, with proper consideration of both the internal state of the body and the boundary effects at the surfaces. Two types of critical speeds are investigated, namely the one at which the free vibrations become unstable and the one at which the forced vibration of a rotating ring subjected to a constant stationary point load experiences resonance. A comparison is presented of the predictions of the developed model to those of the lower order theories. It is shown that even for thin rings on elastic foundation, high order corrections, beyond the ones of the Timoshenko theory, need to be considered for an accurate estimation of the critical speeds of rotating rings. The new high-order model is superior to the existing ring models in predicting dynamic behaviour of either stationary or rotating rings. Without loss of generality, the model is applicable to both plane strain and plane stress configurations.

Keywords: Rotating ring on elastic foundation, Geometrical nonlinearity, In-plane vibrations, Through-thickness stress variation, High order model, Boundary effects, Critical speeds

---

[*]Corresponding author.
Email address: `T.Lu-2@tudelft.nl` (T. Lu)

1. Introduction

The vibration of rotating rings on an elastic foundation is a classical topic in solid mechanics. Various models have been developed after the first work accomplished by Bryan in 1890 [1]. The studies on the rotating ring dynamics thrived in the field of tyre research approximately half a century ago when such models were widely used to describe the in-plane vibrations of the pneumatic tyres [2–4]. The research on tyres using rotating rings is still ongoing [5–8] despite the availability of detailed finite element models. Other applications of rotating rings include flywheel energy storage systems [9], rate sensors [10], flexible train wheels [11, 12] and compliant gears [13]. Most studies to date focus on the in-plane vibrations of rotating thin rings, in which classical low-order theories apply [2–7, 13–15]. Attention to other aspects has been paid as well, among which are the influence of shear deformation and rotatory inertia [16–18], out-of-plane vibrations [10, 19], and nonlinear vibrations [20, 21].

In the references mentioned above, the equations of motion were derived assuming the inner and outer surfaces of the ring to be traction-free. However, when one considers a ring whose inner surface is elastically restrained by distributed springs, this assumption is violated. The traction force at the inner surface can significantly influence the stress distribution in the ring and affect its dynamics. This is especially important in the case of rings rotating at high speeds and supported by stiff foundation. Besides the neglect of the non-zero tractions at the inner surface, most of the previous studies did not account for the centrifugal force associated with the radial expansion due to rotation. Notable exceptions are the works [13, 18–20], in which nonlinear governing equations are first derived and subsequently linearised around the static equilibrium to obtain the linear dynamic equations of motion.

Although various models exist, the theoretical predictions for critical speeds are in striking disagreement. There are two kinds of critical speeds of interest in the case of a rotating ring. One corresponds to possible instabilities of the divergence type of mode $n = 0$ and flutter type of higher modes (the corresponding ring displacements increase exponentially when applying a set of initial conditions) [22], whereas the other one corresponds to resonances of a rotating ring subjected to a stationary load of constant magnitude. To the authors' knowledge, the onset of instability was not properly addressed in the scientific literature prior to recent publication [22] in which the existence of divergence instability of high-speed rotating ring is thoroughly addressed. Recently, divergence instability of a similar type is theoretically predicted in magnetically levitated rotating rings by Arena and Lacarbonara [23]. The condition of resonance of a stationary ring subjected to a constant moving load is well-known [24, 25]. In contrast, the existence of resonances in the reciprocal problem, namely a rotating ring subjected to a stationary load of constant magnitude, is still debated. The most commonly used Endo-Huang-Soedel model [14, 26, 27] does not predict resonance for a rotating ring subjected to a constant stationary load. Lin and Soedel [17, 28] argued that the incapability of predicting resonance speeds is due to the employment of the Green-Lagrange strain-displacement relation, which causes cancellation of rotation effects. The resonance speeds were investigated including shear deformation and rotatory inertia by Lin and Soedel [28]. However, the linearisation procedure adopted in [28] is discussable. Recent contributions to the discussion on the existence of resonance speeds can be found in [29–31].

In this paper, a new geometrically nonlinear model for rotating rings on elastic foundation is proposed. It is well accepted nowadays that the effect of the rotation-induced hoop stress needs to be incorporated to accurately predict the dynamic behaviour of rotating rings. To capture this effect, a nonlinear strain-displacement relation needs to be employed. However, the choice of

the nonlinear strain-displacement relation is ambiguous in the literature despite the fact that this choice influences the predictions of the dynamic behavior of rings rotating at high speeds. A recent discussion on the influence of the choice of different strain measures on dynamic behaviours of rotating toroidal shells can be found in [32]. In this work, the engineering nonlinear strain-displacement relations are adopted from [33], retaining both the nonlinear circumferential and shear strains. The reason for the choice of engineering strain is clearly explained in [34, 35].

To account for the boundary effects (tractions) at the inner and outer surfaces of the ring, the radial and circumferential displacements are approximated by polynomials, the degree of which can be adjusted to consider different complexity of the deformation pattern. For example, linear polynomials in both radial and circumferential displacements yield the classical low order thin ring theory in which only the displacements at the middle surface of the ring is considered. Retaining more terms yields the Timoshenko-type theory and other higher order theories. By introducing these nonlinear displacement distributions and consequently through-thickness variations of stresses, the influence of the tractions at the inner and outer surfaces of the ring on the internal state of the body are addressed. In contrast, other models available in the literature, e.g. [5, 13, 14, 18, 26, 28], cannot deal with the boundary effects in question. Note that although the influence of boundary effects on the internal body of the ring is treated in a proper manner, the boundary conditions themselves are not strictly satisfied.

The developed high-order model (upon linearisation) is verified by comparing the predicted frequency spectra with those resulting from linear elasticity of the corresponding stationary ring case. It is shown that the high-order theory is superior to the existing classical thin ring model [13] and the Timoshenko-type ring model [18]. Contrary to the most commonly used Endo-Huang-Soedel model [14, 26, 27], the model presented in this paper does predict the existence of resonances of a rotating ring subjected to a stationary load of constant magnitude, as well as instability of free vibrations. This conclusion is based on rigorous analysis and is considered by the authors as a novel contribution of this paper.

To examine the influence of higher order corrections on the critical speeds, predictions of the new model are compared with those obtained using the other models in which the same procedure of obtaining the static equilibrium and the same nonlinear strain-displacement relation are applied. These models are: the classical rotating thin ring model [13], the improved classical model including a through-thickness variation of the radial stress [22], and the Timoshenko-type model [18]. It is shown that in the case of thin rings rotating at a high speed, the classical low-order theory is inapplicable. The effects of shear deformation and rotatory inertia need to be considered, as a minimum, to obtain qualitatively accurate results. Due to these effects, resonances of bending-dominated motions always occur at lower speeds than those of extensional or shear motions. Although the Timoshenko-type theory [18] improves the predictions of critical speeds, it is insufficient when the ring rests on a stiff foundation or rotates at high speeds. The proper considerations of boundary effects at both surfaces and the variation of through-thickness radial and shear stresses are of significance for rings connected to stiff foundation especially when the ring dynamics is governed by the long-wave processes.

The paper is structured as follows. Section 2 deals with the derivation of the high-order nonlinear governing equations. Subsequently, linearisation is accomplished around the static equilibrium considering the nonlinear equations. The proposed model can deal with both plane strain and plane stress situations by adjusting a single parameter. The applicability of high-order theory is examined in Section 3 for the stationary ring case. Critical speeds predicted by the proposed model are compared with those predicted by other models in Section 4. Finally, Section 5 summarises all the important conclusions of this paper.
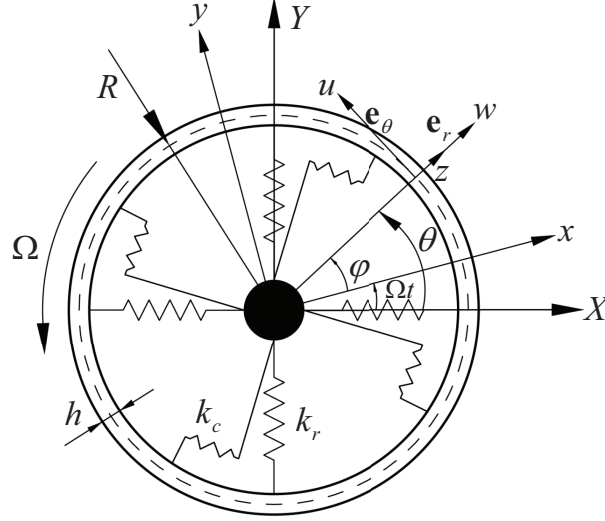
Figure 1: A rotating ring on an elastic foundation

2. High-order rotating ring model

2.1. Derivation of the nonlinear governing equations

In this section, the governing equations of a rotating ring of rectangular cross-section are derived taking into account the through-thickness variation of displacements and stresses. The model under consideration is shown in Fig. 1. It consists of a flexible rotating ring and distributed radial and circumferential springs that connect the inner surface of the ring to an immovable axis. The ring rotates at an angular speed Ω. To describe the motion of a differential element of the ring, one can use either a coordinate system that rotates at angular speed Ω or a space-fixed, non-rotating coordinate system. In this paper, a space-fixed coordinate system (r, θ) is adopted.

It is assumed that the mean radius of the ring is R. To simplify mathematical expressions, an auxiliary coordinate z is introduced as $z = r - R$, in which r defines the radial coordinate, i.e. the ring occupies the space $R - h/2 \leq r \leq R + h/2$, in which h is the radial thickness of the ring. The radial and circumferential displacements of the ring with respect to the undeformed configuration are designated by $w(z, \theta, t)$ and $u(z, \theta, t)$, respectively. The stiffnesses of the radial and circumferential springs per unit area are designated as k_r and k_c (N/m^3), respectively. Furthermore, ρ is the mass density of the ring, E is the Young's modulus, A is the cross-sectional area and I is the cross-sectional moment of inertia. In addition, b is the width of the ring.

The nonlinear strain-displacement relation for the circumferential strain ε_θ, the radial strain ε_r and the shear strain $\gamma_{\theta r}$ of a differential element in the ring are given by [33]

$$
\begin{aligned}
\varepsilon_\theta &= \varepsilon_0 + \frac{1}{2}(\beta)^2, \\
\varepsilon_r &= w_{,r} + \frac{1}{2}(u_{,r})^2, \\
\gamma_{\theta r} &= (1 - w_{,r})u_{,r} - \beta\eta,
\end{aligned}
\tag{1}
$$

4

in which:

$$\varepsilon_0 = \frac{u'}{r} + \frac{w}{r}, \ \beta = \frac{u}{r} - \frac{w'}{r}, \ \eta = 1 - \varepsilon_0,$$

$$u_{,r} = \frac{\partial u}{\partial r} = \frac{\partial u}{\partial z}, \ w_{,r} = \frac{\partial w}{\partial r} = \frac{\partial w}{\partial z}. \tag{2}$$

Hereafter, the prime stands for the partial derivative with respect to θ whereas the subscript $(,r)$ stands for the partial derivative with respect to r. Since $r = R + z$ the derivative with respect to r equals that with respect to z. All strain components are functions of (z, θ, t), e.g. $\varepsilon_\theta \to \varepsilon_\theta(z, \theta, t)$.

The in-plane motions of the ring can either be considered within the plane strain or plane stress formulations, depending on the ring geometry. Without loss of generality, the isotropic linear elastic stress-strain relations can be written as [36]:

$$\begin{Bmatrix} \sigma_r \\ \sigma_\theta \\ \tau_{r\theta} \end{Bmatrix} = \begin{bmatrix} 2\mu + \bar{\lambda} & \bar{\lambda} & 0 \\ \bar{\lambda} & 2\mu + \bar{\lambda} & 0 \\ 0 & 0 & \mu \end{bmatrix} \begin{Bmatrix} \varepsilon_r \\ \varepsilon_\theta \\ \gamma_{r\theta} \end{Bmatrix} \tag{3}$$

in which the coefficient $\bar{\lambda}$ is defined as

$$\bar{\lambda} = \lambda \qquad \qquad \text{(plane strain)}, \tag{4a}$$

$$\bar{\lambda} = \frac{2\mu\lambda}{2\mu + \lambda} = \frac{E\nu}{1 - \nu^2} \qquad \text{(plane stress)} \tag{4b}$$

where λ and μ are the Lamé constants which can be expressed by

$$\lambda = \frac{E\nu}{(1 + \nu)(1 - 2\nu)}, \ \mu = G = \frac{E}{2(1 + \nu)} \tag{5}$$

in terms of Poisson's ratio ν and Young's modulus E and G is the shear modulus.

The velocity vector of a differential element of the ring in the space-fixed frame reads

$$\dot{\mathbf{r}} = [\dot{w} + (w' - u)\Omega] \mathbf{e}_r + [\dot{u} + (r + w + u')\Omega] \mathbf{e}_\theta$$

$$= v_1 \mathbf{e}_r + v_2 \mathbf{e}_\theta. \tag{6}$$

The vectors $\mathbf{e}_r$ and $\mathbf{e}_\theta$ are unit vectors in the radial and circumferential directions, respectively. The overdot represents partial derivative with respect to time.

To derive the equations of motion, the Hamilton's principle is used, i.e.

$$\delta \int_{t_1}^{t_2} (S + V - T)\, \mathrm{d}t = \int_{t_1}^{t_2} (\delta S + \delta V - \delta T)\, \mathrm{d}t = 0 \tag{7}$$

where S is the strain energy, T is the kinetic energy and V is the potential energy stored in the elastic foundation.

The variation of strain energy is given by

$$\delta S = \delta S_1 + \delta S_2 + \delta S_3 \tag{8}$$

in which δS_1 is the variation of the strain energy associated with circumferential strain, δS_2 is the addition to that due to a non-zero radial strain, and δS_3 is the strain energy related to shear strain.

5

Integrating δS_1 between two time instants, t_1 and t_2, yields

$$
\begin{aligned}
\int_{t_1}^{t_2} \delta S_1 \, dt &= b \int_{t_1}^{t_2} \int_{-h/2}^{h/2} \int_0^{2\pi} (\sigma_\theta \, \delta\varepsilon_\theta) r \, d\theta dz dt \\
&= b \int_{t_1}^{t_2} \int_{-h/2}^{h/2} \int_0^{2\pi} \sigma_\theta \, \delta[\varepsilon_0 + \frac{1}{2}(\beta)^2] r \, d\theta dz dt \\
&= b \int_{t_1}^{t_2} \int_{-h/2}^{h/2} \int_0^{2\pi} \sigma_\theta(\delta\varepsilon_0 + \beta \, \delta\beta) r \, d\theta dz dt \\
&= b \int_{t_1}^{t_2} \int_{-h/2}^{h/2} \int_0^{2\pi} \{ [\sigma_\theta + (\sigma_\theta \beta)'] \delta w \\
&\quad - [(\sigma_\theta)' - \sigma_\theta \beta] \delta u \} \, d\theta dz dt \\
&\quad + b \int_{t_1}^{t_2} \int_{-h/2}^{h/2} \left[(\sigma_\theta \delta u) \big|_0^{2\pi} - (\sigma_\theta \beta \delta w) \big|_0^{2\pi} \right] dz dt.
\end{aligned}
\tag{9}
$$

The last integral in Eq. (9) vanishes because the displacements at $\theta = 0$ and at $\theta = 2\pi$ are equal.

The integration of δS_2 from t_1 to t_2 gives

$$
\begin{aligned}
\int_{t_1}^{t_2} \delta S_2 \, dt &= b \int_{t_1}^{t_2} \int_{-h/2}^{h/2} \int_0^{2\pi} (\sigma_r \, \delta\varepsilon_r) r \, d\theta dz dt \\
&= b \int_{t_1}^{t_2} \int_{-h/2}^{h/2} \int_0^{2\pi} \sigma_r \, \delta[w_{,r} + \frac{1}{2}(u_{,r})^2] r \, d\theta dz dt \\
&= b \int_{t_1}^{t_2} \int_{-h/2}^{h/2} \int_0^{2\pi} (r\sigma_r \, \delta w_{,r} + r\sigma_r \, u_{,r} \, \delta u_{,r}) \, d\theta dz dt \\
&= -b \int_{t_1}^{t_2} \int_{-h/2}^{h/2} \int_0^{2\pi} [(r\sigma_r)_{,r} \, \delta w + (r\sigma_r \, u_{,r})_{,r} \, \delta u] \, d\theta dz dt \\
&\quad + b \int_{t_1}^{t_2} \int_0^{2\pi} \left[(r \, \sigma_r \delta w) \big|_{-h/2}^{h/2} + (r \, \sigma_r \, u_{,r} \delta u) \big|_{-h/2}^{h/2} \right] d\theta dt
\end{aligned}
\tag{10}
$$

6

The integration of δS_3 from t_1 to t_2 reads

$$
\begin{aligned}
\int_{t_1}^{t_2} \delta S_3 \, dt &= b \int_{t_1}^{t_2} \int_{-h/2}^{h/2} \int_0^{2\pi} (\tau_{\theta r} \, \delta\gamma_{\theta r}) r \, d\theta dz dt \\
&= b \int_{t_1}^{t_2} \int_{-h/2}^{h/2} \int_0^{2\pi} \tau_{\theta r} \, \delta[u_{,r}(1 - w_{,r}) - \beta\eta] r \, d\theta dz dt \\
&= b \int_{t_1}^{t_2} \int_{-h/2}^{h/2} \int_0^{2\pi} \Big\{ r\tau_{\theta r}(1 - w_{,r})\delta u_{,r} - r\tau_{\theta r} u_{,r} \delta w_{,r} \\
&\quad + r \Big[\frac{\tau_{\theta r}\beta}{r} - \frac{(\tau_{\theta r}\eta)'}{r} \Big] \delta w - r \Big[\frac{\tau_{\theta r}\eta}{r} + \frac{(\tau_{\theta r}\beta)'}{r} \Big] \delta u \Big\} d\theta dz dt \\
&= b \int_{t_1}^{t_2} \int_{-h/2}^{h/2} \int_0^{2\pi} \Big\{ [\tau_{\theta r}\beta - (\tau_{\theta r}\eta)' + (r\tau_{\theta r}u_{,r})_{,r}]\delta w \\
&\quad - [\tau_{\theta r}\eta + (\tau_{\theta r}\beta)' + (r\tau_{\theta r}(1 - w_{,r}))_{,r}]\delta u \Big\} d\theta dz dt \\
&\quad + b \int_{t_1}^{t_2} \int_0^{2\pi} \Big\{ (-\tau_{\theta r}u_{,r}\, \delta w)\Big|_{-h/2}^{h/2} + [r\tau_{\theta r}(1 - w_{,r})\delta u]\Big|_{-h/2}^{h/2} \Big\} d\theta dt \\
&\quad + b \int_{t_1}^{t_2} \int_{-h/2}^{h/2} [(\tau_{\theta r}\beta \, \delta u)\big|_0^{2\pi} + (\tau_{\theta r}\eta \, \delta w)\big|_0^{2\pi}] dz dt.
\end{aligned}
\tag{11}
$$

The last integral in Eq. (11) over time and z vanishes due to the equivalence of the displacements and stresses at $\theta = 0$ and at $\theta = 2\pi$.

Integration over time of the kinetic energy variation can be evaluated as

$$
\begin{aligned}
\int_{t_1}^{t_2} \delta T \, dt &= \frac{\rho b}{2} \int_{t_1}^{t_2} \int_{-h/2}^{h/2} \int_0^{2\pi} \delta(\dot{\mathbf{r}} \cdot \dot{\mathbf{r}}) r \, d\theta dz dt \\
&= \frac{\rho b}{2} \int_{t_1}^{t_2} \int_{-h/2}^{h/2} \int_0^{2\pi} \delta(v_1^2 + v_2^2) r \, d\theta dz dt \\
&= \frac{\rho b}{2} \int_{t_1}^{t_2} \int_{-h/2}^{h/2} \int_0^{2\pi} (2v_1 \, \delta v_1 + 2v_2 \, \delta v_2) r \, d\theta dz dt \\
&= \rho b \int_{t_1}^{t_2} \int_{-h/2}^{h/2} \int_0^{2\pi} [(-\dot{v}_1 - \Omega v_1' + v_2 \Omega)\delta w \\
&\quad - (\dot{v}_2 + \Omega v_2' + v_1 \Omega)\delta u] r \, d\theta dz dt
\end{aligned}
\tag{12}
$$

in which v_1 and v_2 are given in Eq. (6).

The variation of the potential energy due to the elastic foundation is given by

$$
\delta V = \delta V_1 + \delta V_2
\tag{13}
$$

in which δV_1 is related to the potential energy stored in the radial springs which connect the inner surface of the ring to its hub while δV_2 to that of the tangential springs. The integration over time of δV_1 and δV_2 yields

$$
\int_{t_1}^{t_2} \delta V_1 \, dt = b \int_{t_1}^{t_2} \int_0^{2\pi} \Big[(k_r w r \, \delta w)\big|_{z=-h/2} \Big] d\theta dt
\tag{14}
$$

7

and

$$\int_{t_1}^{t_2} \delta V_2 \, \mathrm{d}t = b \int_{t_1}^{t_2} \int_0^{2\pi} \left[(k_c \, u \, r \, \delta u) \big|_{z=-h/2} \right] \mathrm{d}\theta \mathrm{d}t. \tag{15}$$

Upon substitutions of Eqs. (9-15) to Eq. (7) and after consideration of variational calculus, the governing equations are obtained.

First, after substitutions of Eqs. (9-15) to Eq. (7), the double integrals which are associated with the effects of the boundaries at $z = \pm h/2$ are collected, i.e.:

$$
\begin{aligned}
& b \int_{t_1}^{t_2} \int_0^{2\pi} \left\{ [(r\,\sigma_r - r\,\tau_{\theta r} u_{,r})\delta w] \big|_{z=h/2} \right\} \mathrm{d}\theta \mathrm{d}t \\
& - b \int_{t_1}^{t_2} \int_0^{2\pi} \left\{ [(r\,\sigma_r - r\,\tau_{\theta r} u_{,r} - k_r\,w\,r)\delta w] \big|_{z=-h/2} \right\} \mathrm{d}\theta \mathrm{d}t \\
& + b \int_{t_1}^{t_2} \int_0^{2\pi} \left\{ [(r\,\sigma_r\,u_{,r} + r\,\tau_{\theta r}(1 - w_{,r}))\delta u] \big|_{z=h/2} \right\} \mathrm{d}\theta \mathrm{d}t \\
& - b \int_{t_1}^{t_2} \int_0^{2\pi} \left\{ [(r\,\sigma_r\,u_{,r} + r\,\tau_{\theta r}(1 - w_{,r}) - k_c\,u\,r)\delta u] \big|_{z=-h/2} \right\} \mathrm{d}\theta \mathrm{d}t \\
& = b \int_{t_1}^{t_2} \int_0^{2\pi} \left(f_1\,\delta w \big|_{z=h/2} - f_2\,\delta w \big|_{z=-h/2} + f_3\,\delta u \big|_{z=h/2} - f_4\,\delta u \big|_{z=-h/2} \right) \mathrm{d}\theta \mathrm{d}t
\end{aligned}
\tag{16}
$$

in which

$$f_1 = \{r\,(\sigma_r - \tau_{\theta r} u_{,r})\} \big|_{z=h/2}, \tag{17a}$$

$$f_2 = \{r\,(\sigma_r - \tau_{\theta r} u_{,r} - k_r\,w)\} \big|_{z=-h/2}, \tag{17b}$$

$$f_3 = \{r\,[\sigma_r\,u_{,r} + \tau_{\theta r}(1 - w_{,r})]\} \big|_{z=h/2}, \tag{17c}$$

$$f_4 = \{r\,[\sigma_r\,u_{,r} + \tau_{\theta r}(1 - w_{,r}) - k_c\,u]\} \big|_{z=-h/2}. \tag{17d}$$

Second, the displacement fields are expressed as polynomials in both radial and circumferential directions:

$$w(z,\theta,t) = \sum_{l=0}^{l=N_1} w_l(\theta,t)\,z^l, \quad u(z,\theta,t) = \sum_{q=0}^{q=N_2} u_q(\theta,t)\,z^q \tag{18}$$

in which l, q are integers and $l \geq 0$, $q \geq 0$. This results at

$$\delta w = \sum_{l=0}^{l=N_1} \delta w_l\,z^l, \quad \delta u = \sum_{q=0}^{q=N_2} \delta u_q\,z^q \tag{19}$$

and

$$\delta w \big|_{z=\pm h/2} = \sum_{l=0}^{l=N_1} \delta w_l\,(\pm h/2)^l, \quad \delta u \big|_{z=\pm h/2} = \sum_{q=0}^{q=N_2} \delta u_q\,(\pm h/2)^q. \tag{20}$$

Combining Eqs. (7-20) and collecting coefficients of δw_l and δu_q, the nonlinear governing equations can be obtained by setting the coefficients of δw_l and δu_q equal to zero. The equations

8

of motion (the coefficient of δw_l, contains $N_1 + 1$ equations) that govern the dynamic equilibrium in the radial direction read

$$\int_{\frac{-h}{2}}^{\frac{h}{2}} (\mathrm{I}_1 \, z^l) \, dz + \rho \int_{\frac{-h}{2}}^{\frac{h}{2}} [r(\dot{v}_1 + \Omega \, v'_1 - \Omega \, v_2)z^l] \, dz + \left[f_1 - f_2(-1)^l \right] \left(\frac{h}{2} \right)^l = 0, \tag{21}$$
$$(l = 0, 1, 2, 3...N_1).$$

The equations of motion (the coefficient of δu_q, contains $N_2 + 1$ equations) that govern the circumferential equilibrium are given as

$$\int_{\frac{-h}{2}}^{\frac{h}{2}} (\mathrm{I}_2 \, z^q) \, dz + \rho \int_{\frac{-h}{2}}^{\frac{h}{2}} [r(\dot{v}_2 + \Omega \, v'_2 + \Omega \, v_1)z^q] \, dz + \left[f_3 - f_4(-1)^q \right] \left(\frac{h}{2} \right)^q = 0, \tag{22}$$
$$(q = 0, 1, 2, 3...N_2)$$

in which

$$\mathrm{I}_1 = \sigma_\theta + (\sigma_\theta \beta)' - (r \, \sigma_r)_{,r} - (\tau_{\theta r} \, \eta)' + \tau_{\theta r} \beta + (r \, u_{,r} \, \tau_{\theta r})_{,r}, \tag{23a}$$
$$\mathrm{I}_2 = -(\sigma_\theta)' + \sigma_\theta \beta - (r \, \sigma_r \, u_{,r})_{,r} - \tau_{\theta r} \, \eta - (\tau_{\theta r} \beta)' - \left[r \, \tau_{\theta r}(1 - w_{,r}) \right]_{,r}. \tag{23b}$$

The Eqs. (21-22) present the new mathematical description of the dynamics of a rotating ring on an elastic foundation that takes into account the effect of the tractions on the boundaries of the ring.

Up to now, the derivation is generic and one may truncate the number of terms in Eq. (18) as deemed appropriate. For instance, if one retains w_0, u_0 and u_1 in the series expansion in Eq. (18), the Timoshenko-type model is obtained and a shear correction coefficient needs to be introduced [18]. When one chooses a higher truncation limit, no shear correction coefficient needs to be introduced separately because the proper distribution of shear stress is considered implicitly by the model. This is the same as in the Carrera unified formulation [37–40].

2.2. Static equilibrium

To derive the linear governing equations, the static equilibrium needs to be obtained first from the nonlinear equations. As shown in [13, 22] an angle-independent static equilibrium will be reached when the ring rotates at a constant angular velocity. The static expansion $w_e(z)$ of the ring can be found by substitution of

$$w(z, \theta, t) = w_e(z) = \sum_{l=0}^{l=N_1} w_{el} \, z^l, \tag{24}$$
$$u(z, \theta, t) = 0$$

into the governing equations, i.e. Eqs. (21-22). Upon substitution, the following $N_1 + 1$ equations can be used to determine w_{el}:

$$\int_{\frac{-h}{2}}^{\frac{h}{2}} (\mathrm{I}_1^0 \, z^l) \, dz - \rho \int_{\frac{-h}{2}}^{\frac{h}{2}} r \, \Omega^2(r + w_e)z^l \, dz + \left[f_1^0 - f_2^0(-1)^l \right] \left(\frac{h}{2} \right)^l = 0, \tag{25}$$

9

where

$$I_1^0 = 2\mu\left(\frac{w_e}{r} - \frac{\partial w_e}{\partial r}\right) - r\left[(2\mu + \bar{\lambda})\left(\frac{\partial^2 w_e}{\partial r^2}\right) + \frac{\bar{\lambda}}{r}\frac{\partial w_e}{\partial r}\right],$$

$$f_1^0 = \left\{\left[(2\mu + \bar{\lambda})\frac{\partial w_e}{\partial r} + \bar{\lambda}\frac{w_e}{r}\right]r\right\}\Big|_{z=h/2}, \tag{26}$$

$$f_2^0 = \left\{\left[(2\mu + \bar{\lambda})\frac{\partial w_e}{\partial r} + \bar{\lambda}\frac{w_e}{r} - k_r w_e\right]r\right\}\Big|_{z=-h/2}.$$

Each w_{el} of the total $N_1 + 1$ terms can be obtained separately as a function of the rotational speed Ω. Subsequently, $w_e(z)$ is obtained by applying Eq. (24).

2.3. Linearised equations of motion

Considering small vibrations around the static equilibrium, the displacements can be expressed as

$$w(z, \theta, t) = w_d(z, \theta, t) + w_e(z) = \sum_{l=0}^{l=N_1} w_{dl}(\theta, t) z^l + \sum_{l=0}^{l=N_1} w_{el} z^l,$$

$$u(z, \theta, t) = u_d(z, \theta, t) = \sum_{q=0}^{q=N_2} u_{dq}(\theta, t) z^q, \tag{27}$$

in which all time dependent terms are assumed small. The linearised governing equations are obtained by dropping all the nonlinear terms in Eqs. (21-22).

Linearising Eq. (21), the equations of motion that govern the small vibrations about the static equilibrium in the radial direction read

$$\int_{\frac{-h}{2}}^{\frac{h}{2}} (I_1^{lin} z^l)\, \mathrm{d}z + \rho \int_{\frac{-h}{2}}^{\frac{h}{2}} \left[r(\dot{v}_1 + \Omega v_1' - \Omega v_2)z^l\right]\, \mathrm{d}z + \left[f_1^{lin} - f_2^{lin}(-1)^l\right]\left(\frac{h}{2}\right)^l = 0, \tag{28}$$

The linearised equations of motion in the circumferential direction are given as

$$\int_{\frac{-h}{2}}^{\frac{h}{2}} (I_2^{lin} z^q)\, \mathrm{d}z + \rho \int_{\frac{-h}{2}}^{\frac{h}{2}} \left[r(\dot{v}_2 + \Omega v_2' + \Omega v_1)z^q\right]\, \mathrm{d}z + \left[f_3^{lin} - f_4^{lin}(-1)^q\right]\left(\frac{h}{2}\right)^q = 0. \tag{29}$$

after linearisation of Eq. (22). In Eqs. (28-29),

$$I_1^{lin} = \sigma_\theta^{lin} + \sigma_\theta^0(\beta)' - (r\,\sigma_r^{lin})_{,r} - [(\tau_{\theta r}\,\eta)']^{lin}, \tag{30a}$$

$$I_2^{lin} = -(\sigma_\theta^{lin})' + \sigma_\theta^0\beta - \left[r(\sigma_r^0)u_{,r}\right]_{,r} - (\tau_{\theta r}\,\eta)^{lin} - \left\{\left[r\,\tau_{\theta r}(1 - w_{,r})\right]_{,r}\right\}^{lin}, \tag{30b}$$

$$f_1^{lin} = \left[r(2\mu + \bar{\lambda})\frac{\partial w}{\partial r} + \bar{\lambda}(u' + w)\right]\Big|_{z=h/2}, \tag{30c}$$

$$f_2^{lin} = \left[r(2\mu + \bar{\lambda})\frac{\partial w}{\partial r} + \bar{\lambda}(u' + w) - k_r w\, r\right]\Big|_{z=-h/2}, \tag{30d}$$

$$f_3^{lin} = \left\{\frac{G(r - w_e)(1 - w_{e,r})}{r}(w' - u) + \left[Gr(1 + (w_{e,rr})^2) + \bar{\lambda}(rw_{e,r} + w_e)\right]u_{,r}\right\}\Big|_{z=h/2}, \tag{30e}$$

$$f_4^{lin} = \left\{\frac{G(r - w_e)(1 - w_{e,r})}{r}(w' - u) + \left[Gr(1 + (w_{e,rr})^2) + \bar{\lambda}(rw_{e,r} + w_e)\right]u_{,r} - k_c u\, r\right\}\Big|_{z=-h/2}. \tag{30f}$$

10

The expressions with superscript *lin* are the linearised versions of the earlier introduced nonlinear expressions. The stresses σ_r^0 and σ_θ^0 are caused by rotation and can be found in Appendix A. For brevity, in all the expressions above, w and u stand for w_d and u_d, respectively. The velocities v_1 and v_2 are now related solely to the vibrational velocities, namely

$$v_1 = \left[\dot{w}_d + (w_d' - u_d)\Omega\right], \; v_2 = \left[\dot{u}_d + (u_d' + w_d)\Omega\right]. \tag{31}$$

To obtain the characteristic equation one needs to first substitute

$$w_{dl}(\theta, t) = W_{dl}\, e^{in\theta + i\omega t}, \; u_{dq}(\theta, t) = U_{dq}\, e^{in\theta + i\omega t}, \; (l = 0, 1, 2, 3...N_1, q = 0, 1, 2, 3...N_2), \tag{32}$$

into Eqs. (28-29). In Eq. (32) ω is the natural frequency in space-fixed reference system, n is the circumferential mode number and $i = \sqrt{-1}$. This substitution yields the following matrix equation

$$\mathbf{Da = 0} \tag{33}$$

in which $\mathbf{a} = [W_0, W_1, ..., W_{N_1}, U_0, U_1, ..., U_{N_2}]^T$ and $\mathbf{D}$ is the coefficient matrix of order $(N_1 + N_2 + 2) \times (N_1 + N_2 + 2)$. The characteristic equation can be obtained by setting the determinant of the coefficient matrix equal to zero:

$$f(\omega, n, \Omega) = \det \langle \mathbf{D} \rangle = 0. \tag{34}$$

In this paper, no approximations are introduced for the integrations along the thickness coordinate "z". Instead, the exact integral form of the governing equations is considered.

To derive the non-dimensional form of the governing equations, the following dimensionless parameters are introduced [41]:

$$\begin{aligned} &k = \sqrt{EI/(EA)}, \; \bar{k} = k/R, \; \bar{\gamma} = n\bar{k}, \; \bar{\omega} = \omega k/c_0, \; \bar{v} = R\Omega/c_0, \\ &(\bar{k}_r, \bar{k}_c) = (k_r, k_c)k^2/(Eh), \; W_{0e} = w_{0e}/R, \end{aligned} \tag{35}$$

in which $c_0 = \sqrt{E/\rho}$ is the speed of the longitudinal wave in the rod, $I = bh^3/12$ is the cross section area moment of inertia and $\bar{k}$ is the non-dimensional radius of gyration. Thus, the dimensionless form of the characteristic equation Eq. (34) reads

$$f(\bar{\omega}, \bar{\gamma}, \bar{v}) = 0. \tag{36}$$

The model developed can deal with both plane strain and plane stress problems by choosing the parameter $\bar{\lambda}$ in Eq. (4). Naturally, the model is also applicable for stationary rings when $\Omega = 0$.

3. Applicability of the present model: the case of a stationary ring

In this section, the applicable wavenumber range of the present high-order model is examined. Predictions using the classical ring model [13], the Timoshenko-type model [18] and the model presented in this paper are compared with the exact solution obtained from elasticity theory for $\Omega = 0$ (stationary ring case). A comparison of the stationary ring case suffices for the following reason. Once it is shown that boundary effects are important for stationary rings, one may conclude that the latter will also be of importance for rotating rings since the tractions at the inner surface in the latter case are larger than those of the stationary ring case.

11

3.1. Three qualitatively different wave dispersion characteristics of stationary thin rings on elastic foundation

Before proceeding to the high order theory, the classical theory of thin rings on elastic foundation is briefly reviewed. For the classical theory, only the in-plane flexural and extensional motions are considered. Based on the classical thin ring theory, there are three qualitatively dif-
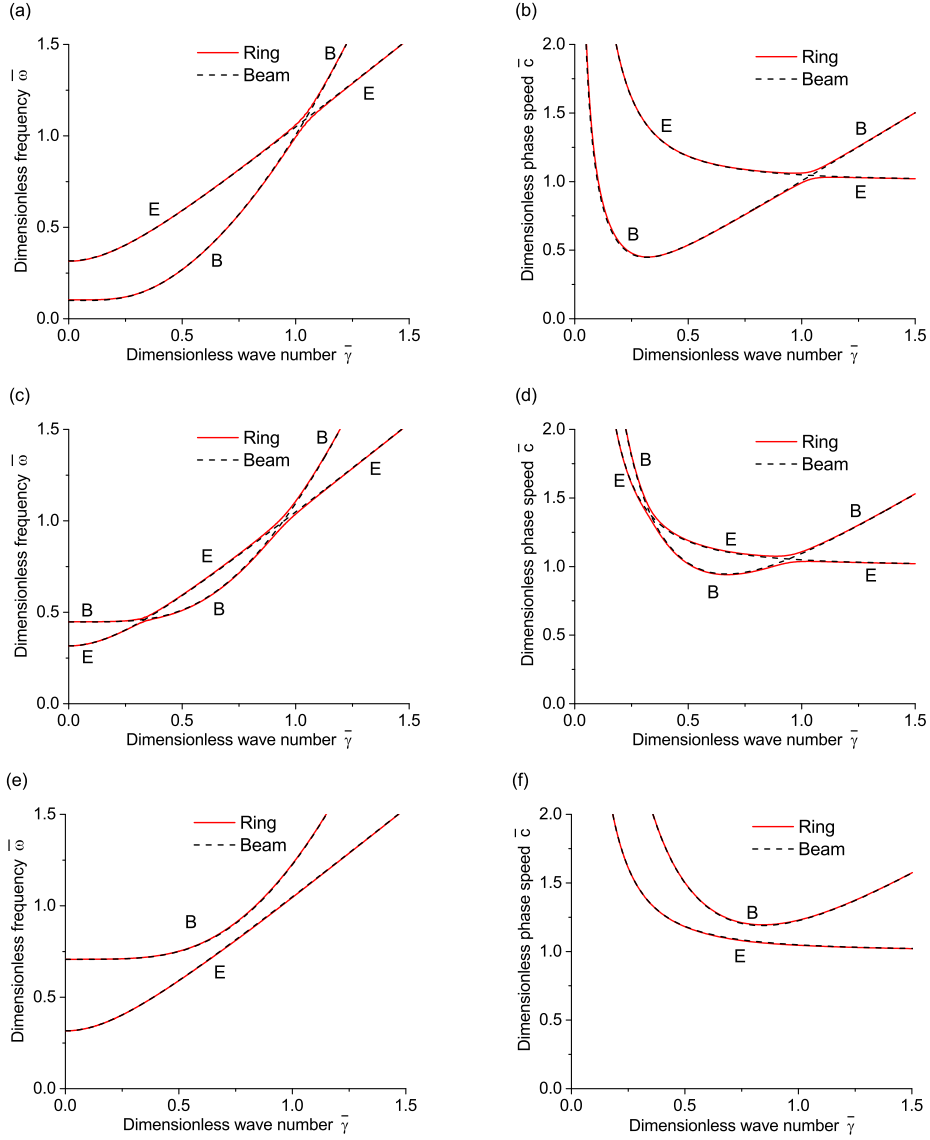

Figure 2: Frequency-wavenumber (left) and phase speed-wavenumber (right) dependencies for $h/R = 0.1, \bar{k}_c = 0.1$: (a)(b) $\bar{k}_r = 0.01$; (c)(d) $\bar{k}_r = 0.2$; (e)(f) $\bar{k}_r = 0.5$. Note that the wavenumber ranges in the plots exceed the applicable range of the classical theory. However, the range is kept for the convenience of explanation.

12

ferent dispersive characteristics, depending on the foundation stiffness and the elastic properties of the ring. The presence of elastic foundation alters the cut-off frequencies of the ring and wave dispersion characteristics. The characteristic equation for the classical thin ring on elastic foundation model is

$$(\bar{\omega}^2 - \bar{k}^2 - \bar{\gamma}^4 - \bar{k}_r)(\bar{\omega}^2 - \bar{\gamma}^2 - \bar{k}^2\bar{\gamma}^2 - \bar{k}_c) - (\bar{k}\bar{\gamma}^3 + \bar{k}\bar{\gamma})^2 = 0. \tag{37}$$

Eq. (37) is the one given in [41], except for the terms $\bar{k}_r, \bar{k}_c$ which are related to the elastic foundation. The phase speed-wavenumber curves in Fig. 2(b)(d)(f) are equivalent to the resonance speed-mode number relations of a circumferentially constant moving point load on the same ring if one considers only discrete wavenumbers $\bar{\gamma} = n\bar{k}$ [25]. These three cases are illustrated in Fig. (2). The red solid lines represent rings, and the black dashed lines are related to the corresponding beam cases predicted by Eq. (37) after setting $\bar{k} = 0$ because $R \to +\infty$ for a beam. Note that the corresponding beam consists of the decoupled transverse (bending) and longitudinal (extension) motions as shown by the degenerated Eq. (37) after setting $\bar{k} = 0$. In Fig. 2, the letter "B" in each subplot means bending-dominated motions whereas "E" stands for extension-dominated motions. For all the three cases, $h/R = 0.1$ is used, $\bar{c}$ is the dimensionless phase speed of waves and $\bar{c} = c/c_0$ ($c_0 = \sqrt{E/\rho}$). The assumed parameters fall into the three cases below:

- Case 1: $\bar{k}_c = 0.1, \bar{k}_r = 0.01$

    The bending-dominated motion has lower natural frequencies and phase speeds until $\bar{\gamma} \approx 1$, when frequency veering happens and the eigenfunctions associated with the two frequency branches interchange [42].

- Case 2: $\bar{k}_c = 0.1, \bar{k}_r = 0.2$

    At low wavenumbers, the bending-dominated motion is characterised by higher natural frequencies till frequencies veer at a certain wavenumber. At $\bar{\gamma} \approx 1$, frequencies veer again.

- Case 3: $\bar{k}_c = 0.1, \bar{k}_r = 0.5$

    The bending-dominated motion occurs at higher natural frequencies and has higher phase speeds.

A general observation is that the curvature coupling is weak for thin rings since the dispersion curves of rings are quite close to their corresponding straight beam cases except for frequencies at which curve veering occurs. Consider a straight beam on elastic foundation, the minimum phase speed of the bending motion in the dimensionless form is [43]

$$\bar{c}_{min} = \sqrt[4]{4k_r EI/(\rho A)^2}/c_0 = \sqrt[4]{4\bar{k}_r}. \tag{38}$$

The minimum phase speeds of rings of Case 1 and Case 2 can be reasonably well approximated by straight beams using Eq. (38). However, for Case 3, the minimum phase speed obtained by the classical thin ring theory equals to the longitudinal wave speed $\sqrt{E/\rho}$.

Note that the dimensionless values $\bar{k}_r = 0.01$, $\bar{k}_r = 0.2$, $\bar{k}_r = 0.5$ represent stiff foundation with respect to the bending stiffness of the ring itself. For example, $\bar{k}_r = 0.01$ represents a foundation whose stiffness is approximately equal to the Young's modulus of a ring of rectangular cross-section if $h = 0.1$m and $R = 1$m. However, in the context of this paper, $\bar{k}_r = 0.01$, $\bar{k}_r = 0.2$, $\bar{k}_r = 0.5$ will be termed "soft", "medium stiff" and "stiff" when referred to for convenience of description.
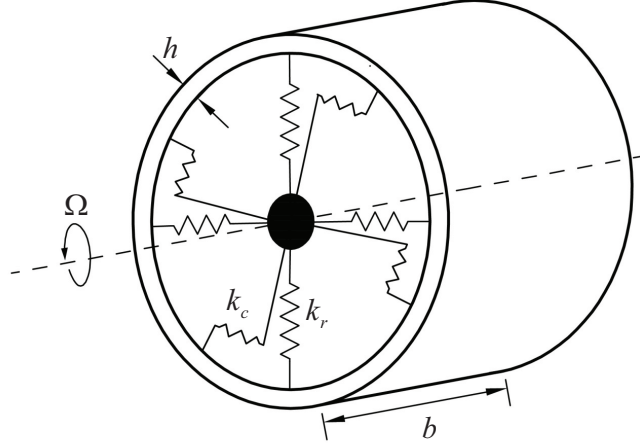
Figure 3: A rotating ring with $b >> h$.

3.2. Comparisons between various ring models and the elasticity theory for a stationary ring

To illustrate the significance of the through-thickness variation of stresses and the boundary effects, the proposed model is compared with the Timoshenko-type model [18] and the two-dimensional elasticity theory for the stationary ring case ($\Omega = 0$). Plane strain is assumed since a ring whose out-of-plane thickness b is much larger than the in-plane thickness h is considered as shown in Fig. 3. For the Timoshenko-type theory, the shear coefficient is adopted from [44]

$$K = \frac{10(1 + \nu)}{12 + 11\nu} \tag{39}$$

for a rectangular cross-section.

The dispersion curves are plotted in Fig. 4 for the three sets of foundation stiffness discussed previously. The two-dimensional elasticity theory employed to obtain the exact solution can be found in Appendix B. Throughout this paper, the Poisson's ratio $\nu = 0.4$ is employed. In each plot of Fig. 4, results obtained from the Timoshenko-type theory [18] consist of three branches, representing bending-dominated motion, extension-dominated motion and shear-dominated motion, respectively. The first four branches of the dispersion curves calculated from the elasticity theory are drawn to compare with the results from the Timoshenko-type theory and the high-order theory proposed in this paper. The truncation orders in Eq. (18) are chosen to be $N_1 = N_2 = 5$.

Comparison of Figs. 2(a)(c)(e) in which the dispersion curves resulting from the classical thin ring model are present, and Fig. 4 shows that the applicability range of the new model is much wider than the existing classical thin ring model [13] and the Timoshenko-type model [18]. The classical thin ring model cannot predict the dispersion curves when the foundation stiffness increases. This also holds for the Timoshenko model the predictions of which deviate significantly from the exact solution for increased foundation stiffness. In contrast, the current model can accurately predict the first four branches of the dispersion curves in the whole range of wavenumbers also in the case of stiff foundation (and thus strong through-thickness variation of the stress components) with the choice of quintic polynomials ($N_1 = N_2 = 5$) for both the
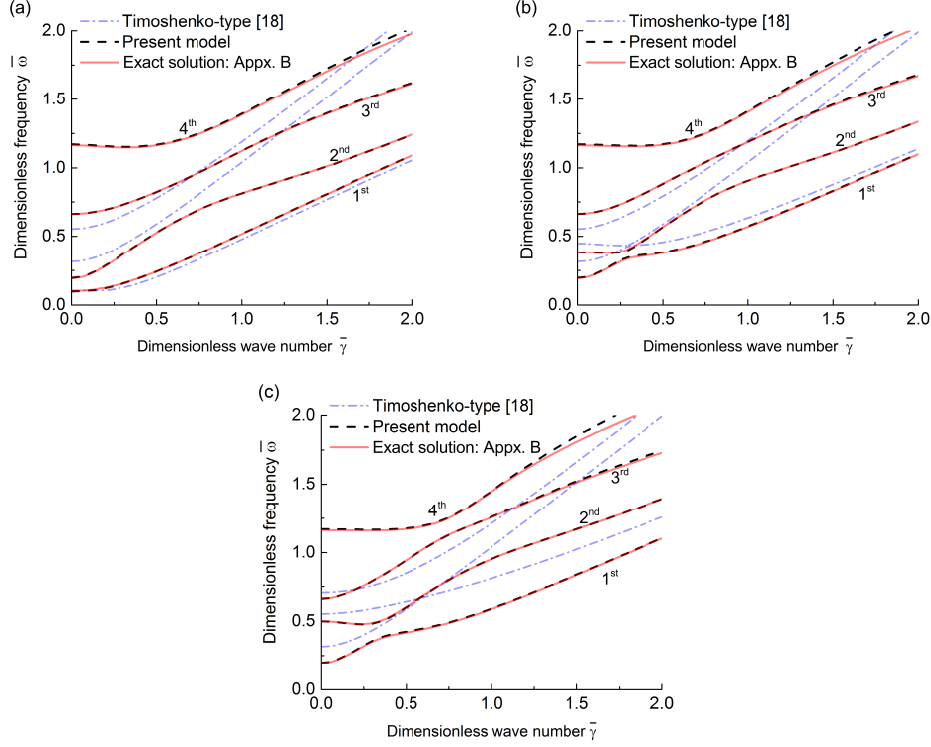
Figure 4: Dispersion curves (plane strain) for $h/R = 0.1$, $\bar{k}_c = 0.1$ and $\Omega = 0$: (a) $\bar{k}_r = 0.01$; (b) $\bar{k}_r = 0.2$; (c) $\bar{k}_r = 0.5$.

radial displacement and circumferential displacement fields. More dispersion curves can be accurately predicted by increasing the degrees of the polynomial displacements accordingly. To conclude, the high-order theory which considers the boundary effects at the surfaces and the through-thickness variations of stresses is shown to be superior to the existing ring models.

4. Critical speeds of rotating rings

In this section, critical speeds of a rotating ring are calculated using different models to illustrate the importance of different factors. As discussed in Section 1, there are two kinds of critical speeds of interest for a rotating ring. One corresponds to possible instability of free vibrations, whereas the other corresponds to resonances of a rotating ring subjected to a stationary load of constant magnitude.

4.1. Applicable rotational speed range

Rotation leads to axi-symmetric radial expansion of the ring. This expansion causes prestress in the ring in both circumferential and radial directions. Thus, there should be a threshold of the rotational speed to avoid the material failure caused by the rotation-induced prestress. As is shown in [22], there are two kinds of prestress which should be examined, namely, the hoop prestress $\sigma_\theta{}^0$ and the radial prestress $\sigma_r{}^0$. The expressions for $\sigma_\theta{}^0$ and $\sigma_r{}^0$ can be found in

15

Appendix A. One should always keep in mind that the model is valid when the material is in the linearly elastic range and therefore the principal stress caused by rotation does not exceed the yield stress.

4.2. Resonance speeds

Resonance speeds are defined as the speeds at which resonances of a rotating ring subjected to a constant stationary load occur, i.e. the speeds which satisfy the condition $\bar{\omega} = 0$ [22, 28, 45, 46]. By substituting $\bar{\omega} = 0$ into the characteristic equation (36), one can solve for the resonance speeds for each circumferential wavenumber. Not that these speeds are altered in the presence of damping and can disappear altogether provided the damping is sufficiently high.

4.2.1. Models considered

In order to illustrate the importance of the boundary effects (non-zero tractions at the inner surface) and through-thickness variation of stresses, predictions made by four models are compared. Table 1 shows the classical thin ring model and the meliorated models with different improvements considered. "R. stress variation" means that the through-thickness variation of radial stress is considered. To achieve this, at least a quadratic polynomial for the radial displacement field is needed. "S. stress variation" stands for the consideration of the through-thickness variation of shear stress. Model 1 is the classical theory [13]; Model 4 is the one developed in this paper. Model 2 [22] accounts for the through-thickness radial stress variation on the basis of the classical ring model. Model 3 is the one adopted from [18] in which the shear deformation and rotatory inertia are included, resulting in a Timoshenko-type model. In analogy to Timoshenko's beam theory, the shear coefficient in Model 3 is given by Eq. (39) for a rectangular cross-section.

4.2.2. Predictions of the various models

The critical speeds of rotating rings are considered in this subsection. The three sets of parameters used to plot Fig. 2 in Section 3 are adopted. In all figures hereafter, the letter "B" means bending-dominated motions, "E" stands for extension-dominated motions, and "S" represents shear-dominated motions. Note that only waves predicted by the lower order Model 1, Model 2 and Model 3 are distinguished in this way. The lower abscissa in each plot is the dimensionless wavenumber, whereas the upper abscissa is the corresponding discrete circumferential mode number. In Figs. 5(d), 6(d) and 7(d), the solid lines correspond to results from the proposed high-order Model 4. For the purpose of comparison, the curves in Figs. 5(d), 6(d) and 7(d) are replicated in Figs. 5(a)(b)(c), 6(a)(b)(c) and 7(a)(b)(c) in grey color.

Figure 5 shows the resonance speeds for $\bar{k}_c = 0.1$ and $\bar{k}_r = 0.01$. Model 1 and Model 2 (Fig. 5(a)(b)) predict quite similar results, indicating that the through-thickness radial stress is not that important. The minimum resonance speed is similar but slightly higher than the minimum phase speed of the corresponding stationary ring case as approximated by Eq. (38) due to stiffening caused by rotation-induced hoop stress. The applicable wavenumber range of Model 1 and Model 2 is lower than $\bar{\gamma} = 0.5$ when compared with the present model (the thick grey lines in Fig. 5(a)(b)) for the chosen parameters. Model 3 and Model 4 predict qualitatively similar resonance speeds for bending-dominated motions as shown in Fig. 5(c). The minimum resonance speeds predicted by Model 3 and Model 4 are similar to those predicted by Model 1 and Model 2. However, Model 4 predicts the highest minimum resonance speed. The resonance speeds of bending-dominated motions approach the Rayleigh wave speed at large wavenumbers. This convergence is reasonable since for the waves whose wavelengths are much shorter than the

16

Table 1: Classical and improved models.

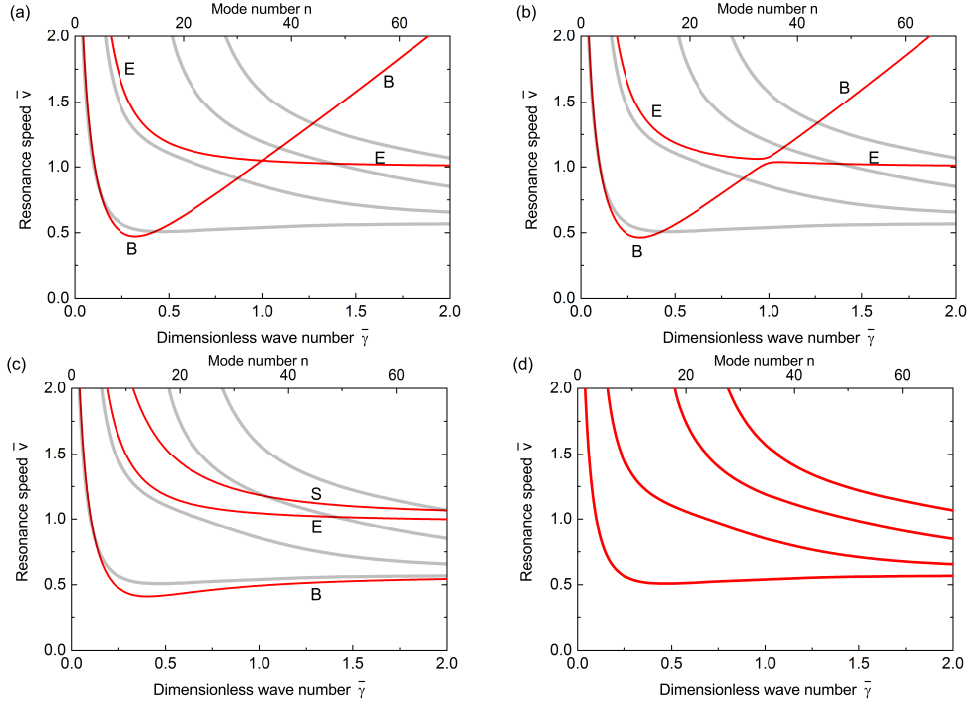| Models	R. stress variation	S. stress variation	Shear deformation	Rotatory inertia	Displacement field Eq. (18)	Static equilibrium
Model 1[13]	×	×	×	×	$N_1 = N_2 = 0$	Refer to [13]
Model 2[22]	✓	×	×	×	$N_1 = 2, N_1 = 0$	Refer to [22]
Model 3[18]	×	×	✓	✓	$N_1 = 0, N_2 = 1$	Refer to [18]
Model 4 (Eqs. (28-29))	✓	✓	✓	✓	$N_1 = N_2 = 5$	Eq. (25)

Figure 5: Resonance speeds for $h/R = 0.1, \bar{k}_c = 0.1, \bar{k}_r = 0.01$: (a) Model 1 (classical model [13]); (b) Model 2 [22]; (c) Model 3 (Timoshenko-type [18]); (d) Model 4 (the present model).

thickness of the ring the effect of the inner boundary disappears. The higher branches (S,E) are not predicted accurately by the Timoshenko-type theory.

To conclude, if the foundation is soft, one can use the classical model to compute the minimum resonance speed although the latter is slightly smaller than the minimum resonance speed predicted by the present model. However, for the resonance speeds of the bending-dominated motions with short wavelengths (high wavenumbers), the first order Timoshenko correction is needed should one be interested in meaningful results. Higher than Timoshenko-type theories are not needed since their predictions are very close to those of the Timoshenko-type theory.

In Figure 6, the stiffness of radial springs is higher than the circumferential one. For this set of parameters, the resonance speeds of bending-dominated motions are larger than those of other branches at low wavenumbers. As the wavenumber increases, both the classical model and Model 2 predict curve veering twice: once at $\bar{\gamma} \approx 1$ and once at a smaller value of $\bar{\gamma}$. Although the classical model (Model 1) and Model 2 predict similar trends, the minimum resonance speed of Model 2 is lower than that of the classical theory. It is shown in Fig. 6(c) and (d) that the shear deformation and rotatory inertia play here a significant role; albeit the contribution of each component is not examined separately. Similar to Model 1 and Model 2, for low wavenumbers, bending-dominated motions have larger resonance speeds. Curves representing flexural and extensional motions veer once at the wavenumber in which the first curve veering occurs in Fig. 6(a) and (b) (the veering is not very obvious in Fig. 6(b) but the curves do veer). Beyond this point, in Fig. 6(c), resonances of shear-dominated motions occur at highest speeds, following
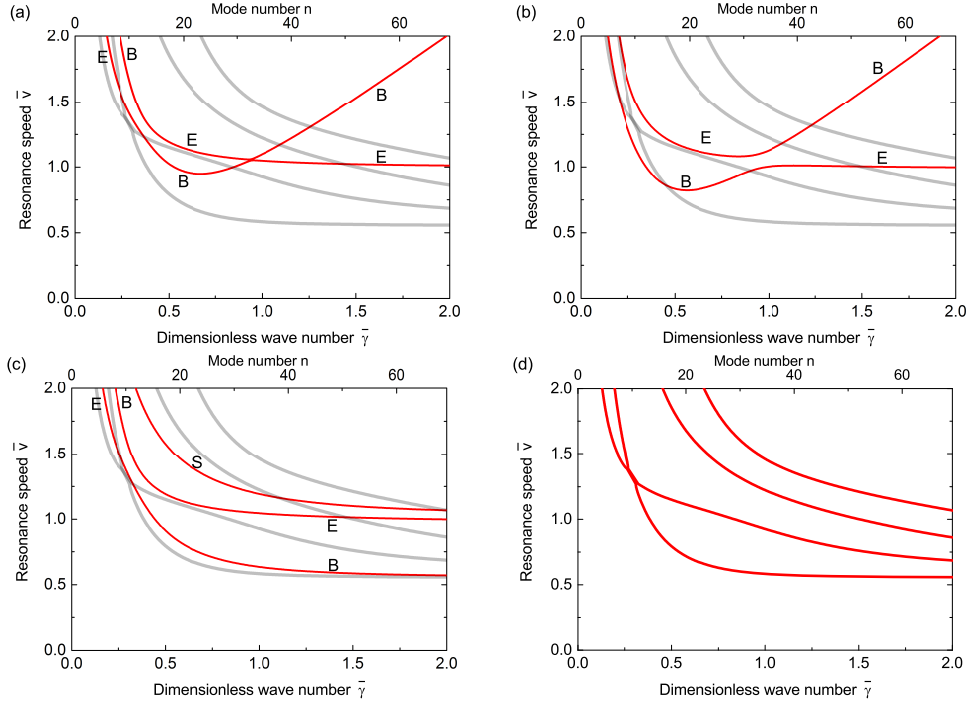
18

Figure 6: Resonance speeds for $h/R = 0.1, \bar{k}_c = 0.1, \bar{k}_r = 0.2$: (a) Model 1 (classical model [13]); (b) Model 2 [22]; (c) Model 3 (Timoshenko-type [18]); (d) Model 4 (the present model).

by extension-dominated motions and bending-dominated motions. Similarly to Fig. 5(c) for the Timoshenko-type model, the Rayleigh surface wave speed is the limit of the bending-dominated motion as is shown in Fig. 6(c). Also, for Model 4, resonance speeds of the lowest wave branch converge to the Rayleigh wave speed. Therefore, if a constant stationary load is applied to the ring and the rotational speed of the ring reaches the Rayleigh wave speed, Rayleigh wave resonance occurs. The Rayleigh wave resonance interpretation is first made by Rabier and Oden in [47] for the standing wave phenomenon in spinning cylinder. Similar conclusions are made by Karttunen and von Hertzen in [48] in which a viscoelastic cylinder cover under rolling contact is considered. It is also shown that for low wavenumbers, the resonance speeds of Fig. 6(d) are different from those of Fig. 6(a)(c) but quite close to Fig. 6(b) in which the radial stress variation along the thickness is considered, implying that this variation is important for waves of relatively long wavelength. Comparing Fig. 6(a), (b), (c) and (d), one can conclude that the lower-order theories are completely inapplicable for medium stiff foundation.

In Figure 7 ($\bar{k}_r/\bar{k}_c = 5$), it is shown that the influence of stress variations increases. The classical theory predicts higher resonance speeds of bending-dominated motions than the extension-dominated motions, and no curve veerings exist. However, when the through-thickness radial stress variation is included in Fig. 7(b), curves veer twice similarly to Fig. 6(b). From the classical theory, the minimum resonance speed corresponding to extensional motions converges to $\sqrt{E/\rho}$. Again for the Timoshenko-type model in Fig. 7(c), the resonance speeds of the bending-dominated motion approach the Rayleigh surface wave speed at high wavenumbers.
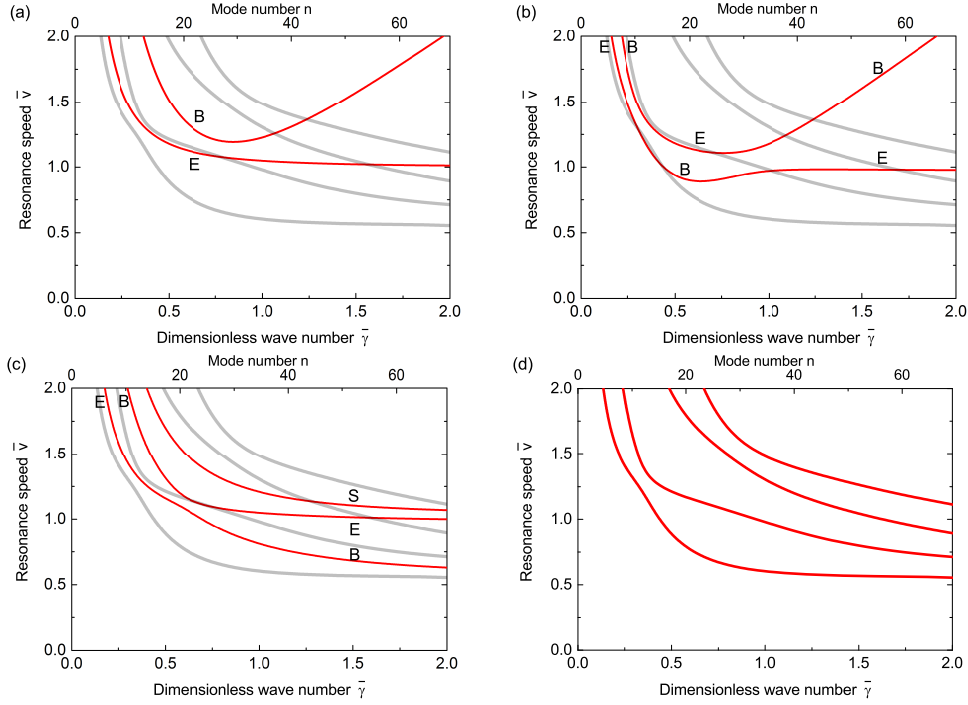
19

Figure 7: Resonance speeds for $h/R = 0.1, \bar{k}_c = 0.1, \bar{k}_r = 0.5$: (a) Model 1 (classical model [13]); (b) Model 2 [22]; (c) Model 3 (Timoshenko-type [18]); (d) Model 4 (the present model).

The quantitatively different resonance speeds predicted in Fig. 7(c) and (d) show the significance of boundary effects and through-thickness variation of stresses for the case of stiff foundation. By observing Fig. 7, it can be seen that the lower-order theories cannot predict the resonance speeds.

For all the three sets of parameters, one can conclude that high order corrections are needed to correctly predict the resonance speeds. For Case 1 in which $\bar{k}_r/\bar{k}_c = 0.1$, the minimum resonance speeds predicted from all models are close. However, when the stiffness of radial springs increases, the minimum resonance speeds predicted by different models are distinct. Shear deformation and rotatory inertia play an important role, as they ensure bending-dominated modes are the ones being always excited at lowest speeds. Although the individual contribution of shear deformation and rotatory inertia are not separately investigated, the observed differences are attributed largely to the effect of shear deformation. The through-thickness variation of stresses and the consideration of boundary effects become significant when $\bar{k}_r/\bar{k}_c$ increases. The consideration of boundary effects on dynamics of the ring is more important for waves with small wavenumbers (long wavelength) than waves of high wavenumbers. It is important to point out that for larger wavenumbers, the resonance speeds of the bending-dominated waves converge to the Rayleigh wave speed. By comparing Fig. 2(b), (d), (f) with Fig. 5(a), Fig. 6(a) and Fig. 7 (a), respectively, it is concluded that for a ring on foundation whose stiffness is of the same order or higher than the Young's modulus, the resonance speeds of a constant load moving circumferentially on the ring and the inverted problem, namely a rotating ring subjected to a constant

20

stationary load, are similar according to the classical thin ring theory. However, due to stress-stiffening, the resonance speeds of rotating ring case are larger than those of the moving load case. In the comparison, the influence of the foundation stiffness in the circumferential direction is not examined since this is expected to be of importance for shear-dominated motion and thus it has limited influence on bending-dominated waves discussed here.

4.2.3. Necessity of high-order theories for rotating rings

As can be concluded from Figs. 5-7, the use of high order theories is important for predicting resonance speeds. Even in the case of soft foundation, the predictions of waves generated are rather different. The predicted resonance speeds change significantly for increasing stiffness of radial springs. This statement holds also for thin rings. For the case of a rotating ring, it is necessary to include high-order corrections, even in the case in which the ring is thin but attached to a stiff foundation. With increasing rotational speeds, the waves excited by a constant stationary load are completely different given the comparison of the predictions by the classical model and the proposed one. For example, comparing Fig. 7(a) and (d), if the ring rotates at $\bar{v} = 0.7$ and is subjected to a constant stationary load, no waves are generated according to the classical model whereas waves will be predicted by the present model.

4.3. Critical speeds associated with the onset of instability

In a previous study [22] of the authors, it has been concluded that the stiffness of the circumferential springs is a key factor influencing the critical speed corresponding to the onset of instability. Lower stiffness of circumferential springs results in lower critical speeds associated with the onset of instability. Here two sets of parameters are chosen; $\bar{k}_r = 0.28$, which corresponds to the stiffness of the radial springs $\bar{K}_r = 4 \times 10^5$ as in [22] and two values of $\bar{k}_c$.
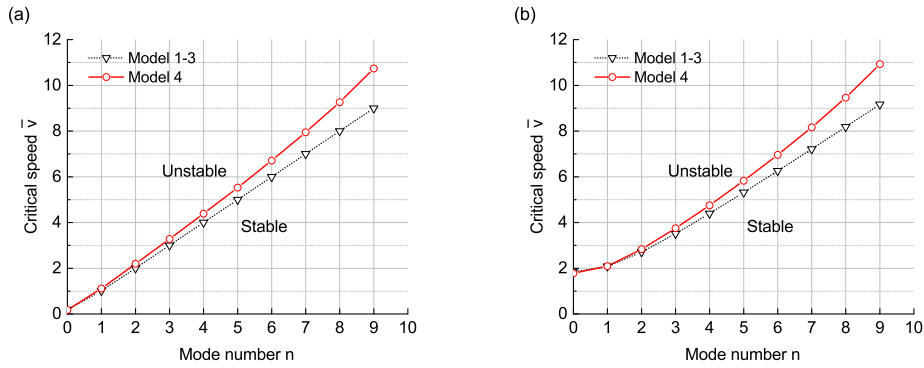

Figure 8: Stability boundaries predicted by different models for $h/R = 0.1$, $\bar{k}_r = 0.28$: (a) $\bar{k}_c/\bar{k}_r = 10^{-4}$; (b) $\bar{k}_c/\bar{k}_r = 10^{-2}$.

The critical speeds corresponding to the onset of instability for different modes (up to $n = 9$) are plotted in Fig. 8 using the models described previously. These speeds divide stable and unstable regions. In Fig. 8, it can be seen that divergence instability of the $n = 0$ rotational mode always occurs at lower rotational speeds compared to flutter of higher modes [22]. The critical speeds obtained from Model 1, Model 2 and Model 3 are quite similar whereas the present model predicts higher critical speeds for mode numbers $n \geq 1$. The differences become larger when the mode number increases. Nevertheless, it can be concluded that the lowest critical speed

21

(corresponding to divergence of $n = 0$) is close regardless of the choice of models. This conclusion is reasonable since higher order corrections influence modes in which elastic deformation dominates.

4.4. On the existence of critical speeds

In the above analysis, the critical speeds calculated from different models are compared. However, it is worth mentioning that for a rotating ring on an elastic foundation, the critical speeds do not always exist. The existence of critical speeds depends on the contribution of the centrifugal softening and stiffening caused by rotation induced prestress. It is argued in [22] that only for a certain combination of stiffnesses of the radial and circumferential springs instability may occur. The stiffness of circumferential springs plays a key role in critical speeds associated with instability. Relatively soft circumferential springs reduce the rotational speeds at which instability occurs. For resonances to occur, stiff radial springs are needed. On the one hand, stiff radial springs impose restrictions on the static expansion due to rotation, and therefore the stress-stiffening effect. The smaller the stiffening effect, the more likely resonances to occur. Meanwhile, if resonances can occur, larger stiffness of radial springs can confine the resonance speeds to those at which the material of the ring is still functioning linearly elastic.

5. Conclusions

In this paper, the in-plane vibration of steadily rotating rings on elastic foundation (distributed springs) is considered. Due to rotation-induced radial expansion, the inner surface which is connected by springs, experiences traction force because of stretching of springs at the static equilibrium. The traction force at the inner surface can be considerably high when the ring rotates at high speeds, resulting in non-negligible through-thickness variations of stresses from non-zero at the inner surface to zero at the outer surface. The same situation also holds for the dynamic forces and stresses at the ring surfaces and in the rings. The classical lower order theories cannot account for either the boundary effects at surfaces or the variations of stresses along the thickness of the ring whereas the developed high-order theory is able to. The present model can precisely describe high order wave motions by increasing the degrees of displacement polynomials.

Two types of critical speeds are discussed. The first one corresponds to resonances of a rotating ring subjected to a constant stationary load. The second one is responsible for instability of the free vibration of a rotating ring. By analysing the critical speeds using different models, it is shown that the higher order corrections are important even for thin rings which are elastically supported. The classical low-order theory becomes inapplicable when the foundation is stiff or when the ring rotates at high speeds. The Timoshenko-type theory performs better when it comes to the prediction of critical speeds, however, it is not accurate for rings rotating at high speed or rings supported by stiff foundation. The influence of boundary effects at the inner and outer surfaces, which are accounted for in the developed model, becomes significant when the foundation is stiff, especially for waves of long wavelength. Regarding the critical speeds associated with instability, if they exist, the developed model predicts higher values than the ones predicted using other models for $n \geq 1$. However, the critical speeds corresponding to $n = 0$ divergence as obtained by different models, are similar.

Acknowledgements

Appendix A. Relation between the rotation induced prestresses and static deformation

From the Hooke's law shown in Eq. (3), the prestress in radial direction is given by

$$\sigma_r{}^0 = 2\mu\,\varepsilon_r{}^0 + \bar{\lambda}\left(\varepsilon_r{}^0 + \varepsilon_\theta{}^0\right) \tag{A.1}$$

and in circumferential direction it reads

$$\sigma_\theta{}^0 = 2\mu\,\varepsilon_\theta{}^0 + \bar{\lambda}\left(\varepsilon_r{}^0 + \varepsilon_\theta{}^0\right) \tag{A.2}$$

where the strains caused by rotation are

$$\varepsilon_r{}^0 = \frac{\partial w_e}{\partial r}, \quad \varepsilon_\theta{}^0 = \frac{w_e}{r} \tag{A.3}$$

in which w_e is given by Eq. (24).

Appendix B. Exact solutions for natural frequencies of the in-plane vibrations of stationary rings

A ring can be considered as a circular annulus. Either plane strain [49] or plane stress [50] assumption can be made according to the examined problem. Assume steady-state time-harmonic waves in the ring, after dropping the time signature $e^{i\omega t}$, the governing equations in polar coordinate (r, θ) are

$$\begin{aligned}
\frac{\partial \sigma_r}{\partial r} + \frac{\sigma_r - \sigma_\theta}{r} + \frac{1}{r}\frac{\partial \tau_{\theta r}}{\partial \theta} + \rho\,\omega^2\,w &= 0, \\
\frac{\partial \tau_{\theta r}}{\partial r} + \frac{1}{r}\frac{\partial \sigma_\theta}{\partial \theta} + \frac{2\,\tau_{\theta r}}{r} + \rho\,\omega^2\,u &= 0
\end{aligned} \tag{B.1}$$

in which $w = w(r,\theta)$, $u = u(r,\theta)$ are the radial and circumferential displacement, respectively. Substituting the Hooke's law Eq. (3) one obtains:

$$\begin{aligned}
\sigma_r &= 2\mu\,\varepsilon_r + \bar{\lambda}\left(\varepsilon_r + \varepsilon_\theta\right) = 2\mu\,\frac{\partial w}{\partial r} + \bar{\lambda}\left(\frac{\partial w}{\partial r} + \frac{w}{r} + \frac{1}{r}\frac{\partial u}{\partial \theta}\right), \\
\sigma_\theta &= 2\mu\,\varepsilon_\theta + \bar{\lambda}\left(\varepsilon_r + \varepsilon_\theta\right) = 2\mu\left(\frac{w}{r} + \frac{1}{r}\frac{\partial u}{\partial \theta}\right) + \bar{\lambda}\left(\frac{\partial w}{\partial r} + \frac{w}{r} + \frac{1}{r}\frac{\partial u}{\partial \theta}\right), \\
\tau_{\theta r} &= \mu\,\gamma_{\theta r} = \mu\left(\frac{\partial u}{\partial r} - \frac{u}{r} + \frac{1}{r}\frac{\partial w}{\partial \theta}\right).
\end{aligned} \tag{B.2}$$

Expression of $\bar{\lambda}$ can be found in Eq. (4).

The Helmholtz decomposition is used to obtain two decoupled governing equations:

$$\nabla^2\hat{\Phi} + \frac{\omega^2}{c_L{}^2}\hat{\Phi} = 0, \quad \nabla^2\hat{H}_z + \frac{\omega^2}{c_T{}^2}\hat{H}_z = 0 \tag{B.3}$$

where $c_L = \sqrt{(\bar{\lambda} + 2\mu)/\rho}$ and $c_T = \sqrt{\mu/\rho}$. The displacements can be expressed as

$$w = \frac{\partial \hat{\Phi}}{\partial r} + \frac{1}{r}\frac{\partial \hat{H}_z}{\partial \theta}, \; u = \frac{1}{r}\frac{\partial \hat{\Phi}}{\partial \theta} - \frac{\partial \hat{H}_z}{\partial r}. \tag{B.4}$$

Applying separation of variables on Eq. (B.3), one will obtain

$$\begin{aligned}
\hat{\Phi}(r, \theta) &= \left(A_n\, J_n(k_p\, r) + B_n\, Y_n(k_p\, r)\right)\cos(n\theta), \\
\hat{H}_z(r, \theta) &= (B_n\, J_n(k_s\, r) + D_n\, Y_n(k_s\, r))\sin(n\theta)
\end{aligned} \tag{B.5}$$

where $k_p = \omega/c_L$ and $k_s = \omega/c_T$; J_n and Y_n are the Bessel functions of the first and second kind, respectively. The boundary conditions are

$$\sigma_r\big|_{-h/2} = k_r\, w\big|_{-h/2}, \;\; \tau_{\theta r}\big|_{-h/2} = k_c\, u\big|_{-h/2} \tag{B.6}$$

at the inner surface and

$$\sigma_r\big|_{h/2} = 0, \;\; \tau_{\theta r}\big|_{h/2} = 0 \tag{B.7}$$

at the outer surface. The frequency equation can be obtained by substituting Eq. (B.5) into the boundary conditions (B.6-B.7).

References

[1] G. Bryan, On the beats in the vibrations of a revolving cylinder or bell, Proceedings of the Cambridge Philosophical Society 7 (1) (1890) 101–111.

[2] J. T. Tielking, Plane vibration characteristics of a pneumatic tire model, SAE Technical Paper 650492, (1965). doi:10.4271/650492.

[3] S. K. Clark, The rolling tire under load, SAE Technical Paper 650493, (1965). doi:10.4271/650493.

[4] F. Böhm, Mechanik des gürtelreifens, Ingenieur-Archiv 35 (1966) 82–101.

[5] S. Gong, A Study of In-Plane Dynamics of Tires, Ph.D. thesis, Delft University of Technology (1993).

[6] Y. Wei, L. Nasdala, H. Rothert, Analysis of forced transient response for rotating tires using REF models, Journal of Sound and Vibration 320 (1) (2009) 145–162. doi:10.1016/j.jsv.2008.07.007.

[7] P. Kindt, P. Sas, W. Desmet, Development and validation of a three-dimensional ring-based structural tyre model, Journal of Sound and Vibration 326 (3) (2009) 852–869. doi:10.1016/j.jsv.2009.05.019.

[8] T. Dai Vu, D. Duhamel, Z. Abbadi, H.-P. Yin, A. Gaudin, A nonlinear circular ring model with rotating effects for tire vibrations, Journal of Sound and Vibration 388 (2017) 245–271. doi:10.1016/j.jsv.2016.10.023.

[9] C. Bert, T. Chen, On vibration of a thick flexible ring rotating at high speed, Journal of Sound and Vibration 61 (4) (1978) 517–530. doi:10.1016/0022-460X(78)90452-2.

[10] R. Eley, C. Fox, S. McWilliam, Coriolis coupling effects on the vibration of rotating rings, Journal of Sound and Vibration 238 (3) (2000) 459–480. doi:10.1006/jsvi.2000.3154.

[11] T. Lu, A. Metrikine, A rotating ring in contact with a stationary load as a model for a flexible train wheel, in: EURODYN 2014: Proceedings of the 9th International Conference on Structural Dynamics, Faculty of Engineering of University of Porto, 2014, pp. 3769–3773.

[12] S. Noga, R. Bogacz, T. Markowski, Vibration analysis of a wheel composed of a ring and a wheel-plate modelled as a three-parameter elastic foundation, Journal of Sound and Vibration 333 (24) (2014) 6706–6722. doi:10.1016/j.jsv.2014.07.019.

[13] C. G. Cooley, R. G. Parker, Vibration of high-speed rotating rings coupled to space-fixed stiffnesses, Journal of Sound and Vibration 333 (12) (2014) 2631–2648. doi:10.1016/j.jsv.2014.01.005.

[14] M. Endo, K. Hatamura, M. Sakata, O. Taniguchi, Flexural vibration of a thin rotating ring, Journal of Sound and Vibration 92 (2) (1984) 261–272. doi:10.1016/0022-460X(84)90560-1.

[15] S. Huang, W. Soedel, Effects of Coriolis acceleration on the forced vibration of rotating cylindrical shells, Journal of Applied Mechanics 55 (1988) 231. doi:10.1115/1.3173637.

[16] W. Bickford, E. Reddy, On the in-plane vibrations of rotating rings, Journal of Sound and Vibration 101 (1) (1985) 13–22. doi:10.1016/S0022-460X(85)80034-1.

[17] J. Lin, W. Soedel, On general in-plane vibrations of rotating thick and thin rings, Journal of Sound and Vibration 122 (3) (1988) 547–570. `doi:10.1016/S0022-460X(88)80101-9`.

[18] H. Ding, M. Zhu, Z. Zhang, Y.-W. Zhang, L.-Q. Chen, Free vibration of a rotating ring on an elastic foundation, International Journal of Applied Mechanics 9 (4) (2017) 1750051. `doi:10.1142/S175882511750051X`.

[19] W. Kim, J. Chung, Free non-linear vibration of a rotating thin ring with the in-plane and out-of-plane motions, Journal of Sound and Vibration 258 (1) (2002) 167–178. `doi:10.1006/jsvi.2002.5104`.

[20] R. Zadoks, C. Krousgrill, Complex dynamics in the quadratically non-linear response of a rotating ring with elastic hub, Journal of Sound and Vibration 165 (3) (1993) 385–408. `doi:10.1006/jsvi.1993.1266`.

[21] S. Natsiavas, Dynamics and stability of non-linear free vibration of thin rotating rings, International Journal of Non-Linear Mechanics 29 (1) (1994) 31–48. `doi:10.1016/0020-7462(94)90050-7`.

[22] T. Lu, A. Tsouvalas, A. Metrikine, The in-plane free vibration of an elastically supported thin ring rotating at high speeds revisited, Journal of Sound and Vibration 402 (2017) 203–218. `doi:10.1016/j.jsv.2017.05.013`.

[23] A. Arena, W. Lacarbonara, On the stability of magnetically levitated rotating rings, International Journal of Mechanical Sciences 131-132 (2017) 286–295. `doi:10.1016/j.ijmecsci.2017.07.007`.

[24] A. Metrikine, M. Tochilin, Steady-state vibrations of an elastic ring under a moving load, Journal of Sound and Vibration 232 (3) (2000) 511–524. `doi:10.1006/jsvi.1999.2756`.

[25] G. Forbes, R. Randall, Resonance phenomena of an elastic ring under a moving load, Journal of Sound and Vibration 318 (4) (2008) 991–1004. `doi:10.1016/j.jsv.2008.05.021`.

[26] S. Huang, W. Soedel, Effects of Coriolis acceleration on the free and forced in-plane vibrations of rotating rings on elastic foundation, Journal of Sound and Vibration 115 (2) (1987) 253–274. `doi:10.1016/0022-460X(87)90471-8`.

[27] S. Huang, W. Soedel, Response of rotating rings to harmonic and periodic loading and comparison with the inverted problem, Journal of Sound and Vibration 118 (2) (1987) 253–270. `doi:10.1016/0022-460X(87)90524-4`.

[28] J. Lin, W. Soedel, On the critical speeds of rotating thick or thin rings, Mechanics of Structures and Machines 16 (4) (1988) 439–483. `doi:10.1080/08905458808960272`.

[29] V. V. Krylov, O. Gilbert, On the theory of standing waves in tyres at high vehicle speeds, Journal of Sound and Vibration 329 (21) (2010) 4398–4408. `doi:10.1016/j.jsv.2010.05.001`.

[30] W. Graham, Discussion of 'On the theory of standing waves in tyres at high vehicle speeds' by V.V. Krylov and O. Gilbert, Journal of Sound and Vibration 329 (2010) 4398–4408, Journal of Sound and Vibration 332 (22) (2013) 6029–6031. `doi:10.1016/j.jsv.2013.06.010`.

[31] V. V. Krylov, Commentary on Discussion of 'On the theory of standing waves in tyres at high vehicle speeds' by V.V. Krylov and O. Gilbert, Journal of Sound and Vibration 329 (2010) 4398–4408, Journal of Sound and Vibration 332 (26) (2013) 7290–7292. `doi:10.1016/j.jsv.2013.08.030`.

[32] I. Senjanović, N. Alujević, I. Ćatipović, D. Čakmak, N. Vladimir, Vibration analysis of rotating toroidal shell by the Rayleigh-Ritz method and Fourier series, Engineering Structures 173 (2018) 870–891. `doi:10.1016/j.engstruct.2018.07.029`.

[33] M. Stein, Nonlinear theory for plates and shells including the effects of transverse shearing, AIAA Journal 24 (9) (1986) 1537–1544. `doi:10.2514/3.9477`.

[34] P. Pai, A. Nayfeh, A new method for the modeling of geometric nonlinearities in structures, Computers & Structures 53 (4) (1994) 877–895. `doi:10.1016/0045-7949(94)90376-X`.

[35] P. F. Pai, Highly Flexible Structures: Modeling, Computation, and Experimentation, AIAA, 2007. `doi:10.2514/4.861925`.

[36] H. Matsunaga, Effects of higher-order deformations on in-plane vibration and stability of thick circular rings, Acta Mechanica 124 (1-4) (1997) 47–61. `doi:10.1007/BF01213017`.

[37] E. Carrera, Theories and finite elements for multilayered plates and shells: a unified compact formulation with numerical assessment and benchmarking, Archives of Computational Methods in Engineering 10 (3) (2003) 215–296. `doi:10.1007/BF02736224`.

[38] E. Carrera, A. Pagani, Analysis of reinforced and thin-walled structures by multi-line refined 1d/beam models, International Journal of Mechanical Sciences 75 (2013) 278–287. `doi:10.1016/j.ijmecsci.2013.07.010`.

[39] E. Carrera, M. Filippi, E. Zappino, Laminated beam analysis by polynomial, trigonometric, exponential and zig-zag theories, European Journal of Mechanics-A/Solids 41 (2013) 58–69. `doi:10.1016/j.euromechsol.2013.02.006`.

[40] A. Pagani, M. Boscolo, J. Banerjee, E. Carrera, Exact dynamic stiffness elements based on one-dimensional higher-order theories for free vibration analysis of solid and thin-walled structures, Journal of Sound and Vibration 332 (23) (2013) 6104–6127. `doi:10.1016/j.jsv.2013.06.023`.

[41] K. Graff, Wave Motion in Elastic Solids, Dover Publications, Inc., New York, 1975.

[42] N. Perkins, C. Mote, Comments on curve veering in eigenvalue problems, Journal of Sound and Vibration 106 (3) (1986) 451–463. `doi:10.1016/0022-460X(86)90191-4`.

[43] A. Metrikine, H. Dieterman, Instability of vibrations of a mass moving uniformly along an axially compressed

beam on a viscoelastic foundation, Journal of Sound and Vibration 201 (5) (1997) 567–576. `doi:10.1006/jsvi.1996.0783`.

[44] G. Cowper, The shear coefficient in Timoshenko's beam theory, Journal of Applied Mechanics 33 (2) (1966) 335–340. `doi:10.1115/1.3625046`.

[45] W. Soedel, Vibrations of Shells and Plates, CRC Press, 2004.

[46] T. Lu, A. Metrikine, On the existence of a critical speed of a rotating ring under a stationary point load, in: Proceedings of 43th International Summer School-Conference Advanced Problems in Mechanics (APM), SPBSPU/IPME RAS, St. Petersburg (Russia), June 2015, pp. 237–245.

[47] P. J. Rabier, J. T. Oden, Bifurcation in rotating bodies, Vol. 11, Springer Verlag, 1989.

[48] A. T. Karttunen, R. von Hertzen, A numerical study of traveling waves in a viscoelastic cylinder cover under rolling contact, International Journal of Mechanical Sciences 66 (2013) 180–191. `doi:10.1016/j.ijmecsci.2012.11.006`.

[49] G. Liu, J. Qu, Guided circumferential waves in a circular annulus, Journal of Applied Mechanics 65 (1998) 424–430. `doi:10.1115/1.2789071`.

[50] S. Bashmal, R. Bhat, S. Rakheja, Frequency equations for the in-plane vibration of circular annular disks, Advances in Acoustics and Vibration 2010. `doi:10.1155/2010/501902`.